ORIGINAL ARTICLE

Comparative evaluation of CT-based and respiratory-gated PET/CT-based planning target volume (PTV) in the definition of radiation treatment planning in lung cancer: preliminary results

Luca Guerra · Sofia Meregalli · Alessandra Zorz · Rita Niespolo · Elena De Ponti ·
Federica Elisei · Sabrina Morzenti · Sarah Brenna · Andrea Crespi ·
Gianstefano Gardani · Cristina Messa

Abstract

Purpose The aim of this study was to compare planning target volume (PTV) defined on respiratory-gated positron emission tomography (PET)/CT (RG-PET/CT) to PTV based on ungated free-breathing CT and to evaluate if RG-PET/CT can be useful to personalize PTV by tailoring the target volume to the lesion motion in lung cancer patients.

Methods Thirteen lung cancer patients (six men, mean age 70.0 years, 1 small cell lung cancer, 12 non-small cell lung cancer) who were candidates for radiation therapy were prospectively enrolled and submitted to RG-PET/CT. Ungated free-breathing CT images obtained during a PET/CT study were visually contoured by the radiation oncologist to define standard clinical target volumes (CTV1). Standard PTV (PTV1) resulted from CTV1 with the addition of 1-cm expansion of margins in all directions. RG-PET/CT images were contoured by the nuclear medicine physician and radiation oncologist according to a standardized institutional protocol for contouring gated images. Each CT and PET image of the patient's respiratory cycle phases was contoured to obtain the RG-CT-based CTV (CTV2) and the RG-PET/CT-based CTV (CTV3), respectively. RG-CT-based and RG-PET/CT-based PTV (PTV2 and PTV3, respectively) were then derived from gated CTVs with a margin expansion of 7–8 mm in head to feet direction and 5 mm in anterior to posterior and left to right direction. The portions of gated PTV2 and PTV3 geometrically not encompassed in PTV1 (PTV2 out PTV1 and PTV3 out PTV1) were also calculated.

Results Mean ± SD CTV1, CTV2 and CTV3 were 30.5 ± 33.2, 43.1 ± 43.2 and 44.8 ± 45.2 ml, respectively. CTV1 was significantly smaller than CTV2 and CTV3 ($p = 0.017$ and 0.009 with Student's t test, respectively). No significant difference was found between CTV2 and CTV3. Mean ± SD of PTV1, PTV2 and PTV3 were 118.7 ± 94.1, 93.8 ± 80.2 and 97.0 ± 83.9 ml, respectively. PTV1 was significantly larger than PTV2 and PTV3 ($p = 0.038$ and 0.043 with Student's t test, respectively). No significant difference was found between PTV2 and PTV3. Mean ± SD values of PTV2 out PTV1 and PTV3 out PTV1 were 12.8 ± 25.4 and 14.3 ± 25.9 ml, respectively. The percentage values of PTV2 out PTV1 and PTV3 out PTV1 were not lower than 10 % of PTV1 in 6/13 cases (46.2 %) and than 20 % in 3/13 cases (23.1 %).

Conclusion Our preliminary data showed that RG-PET/CT in lung cancer can affect not only the volume of PTV but also its shape, as demonstrated by the assessment of gated PTVs outside standard PTV. The use of a gating technique is thus

L. Guerra (✉) · F. Elisei · C. Messa
Nuclear Medicine, San Gerardo Hospital, Monza, Italy
e-mail: l.guerra@hsgerardo.org

S. Meregalli · R. Niespolo · G. Gardani
Radiotherapy, San Gerardo Hospital, Monza, Italy

G. Gardani
University of Milan-Bicocca, Milan, Italy

A. Zorz · E. De Ponti · S. Morzenti · A. Crespi
Medical Physics, San Gerardo Hospital, Monza, Italy

S. Brenna
School of Radiation Oncology, University of Milan-Bicocca,
Monza, Italy

C. Messa
Tecnomed Foundation, University of Milan-Bicocca, Milan, Italy

C. Messa
Institute for Bioimaging and Molecular Physiology,
National Research Council, Milan, Italy

crucial for better delineating PTV by tailoring the target volume to the lesion motion in lung cancer patients.

Introduction

Lung cancer is the most common cause of death among oncological diseases. The treatment of choice is surgery, but it is indicated only in patients with a limited stage of the disease. Other therapeutic options are available today, in particular the three modality approach consisting of surgery, chemotherapy and radiotherapy in different scheduling schemes. In this scenario, radiotherapy has a crucial role in lung cancer treatment and the probability of local control is strictly related to the precise delineation of target volumes.

[18]F-Fluorodeoxyglucose (FDG) positron emission tomography (PET) has demonstrated significant value for radiotherapy of lung cancer. The incorporation of PET and PET/computed tomography (CT) data into the radiation treatment planning has recently gained widespread acceptance as it has been shown to improve gross tumour volume (GTV) definition [1–4].

A limitation of PET studies, performed during shallow breathing, is motion artefacts, which can reduce lesion contrast, underestimate the tracer uptake and overestimate the lesion size and thus the metabolic tumour volume (MTV) [5, 6]. Furthermore, if PET/CT scanners are used, the temporal mismatch between the short (in seconds) CT and the long (in minutes) PET scans may cause a spatial misalignment between CT and PET images with consequent errors in attenuation correction maps [7–10].

Respiratory motion can be managed either by motion suppression (deep inspiration breath hold or forced shallow breathing) or motion compensation [11, 12]; the last one includes a respiratory gating technique that typically bins the imaging acquisition to direct or indirect measurement of motion amplitude. In order to overcome the respiratory motion-related artefacts and the uncertainty in planning target volume (PTV) definition, respiratory-gated CT (RG-CT) has been widely evaluated, both from a methodological and a clinical point of view [13–19]. Gated CT is strongly recommended today in PTV definition in lung cancer patients [20] as it can furnish individualized information on lesion motion and allows the use of smaller margins than standard CT [16, 21, 22]. Furthermore, a gated technique has been shown to reduce PTV and to be an effective imaging guidance strategy to personalize the lung cancer treatment [23–25].

RG-PET/CT has been demonstrated as a feasible technique in routine clinical practice by improving image quality, quantification and diagnostic accuracy in the detection of lung lesions [26–28]. Nevertheless, there is a lack of evidence of its usefulness in radiation treatment planning; to date only one paper evaluating its clinical utility in radiation treatment has been published showing that RG-PET/CT may better estimate the extent of tumour motion and, therefore, improve radiation treatment planning [29].

The purpose of the present study was to compare PTV defined on RG-PET/CT to the standard free-breathing CT-based PTV and to evaluate if RG-PET/CT can be useful to personalize PTV by tailoring the target volume to the lesion motion in lung cancer patients.

Materials and methods

Patients

From March 2010 to March 2012, we prospectively enrolled 13 patients (six men, mean age 70.0 years, range 45–88 years) with histologically proven lung cancer [1 small cell lung cancer (SCLC) and 12 non-small cell lung cancer (NSCLC)] who were candidates for radiation therapy. All patients gave their signed informed consent to the study. Clinical workup included ^{18}F-FDG PET/CT and contrast-enhanced (ce) CT in all patients with the addition of mediastinoscopy (1/13 patients, 7.7 %) and bronchoscopy (4/13 patients, 30.8 %) completed within 1 month before the onset of radiation treatment. Clinical stage of the disease was IA–IVA. Of 13 patients, 9 (69.2 %) underwent chemotherapy concurrently (4/9 patients, 44.4 %) or prior to (5/9 patients, 55.6 %) radiation therapy. Radiation treatment was performed with radical intent in 12/13 patients (92.3 %) and as a part of neoadjuvant treatment in 1/13 patients (7.7 %). Of 13 patients, 1 (7.7 %) was referred to treatment for local relapse and the remaining 12/13 patients (92.3 %) for primary disease. In 7/13 cases (53.8 %) volumetric modulated arc therapy was used, whereas 6/13 patients (46.2 %) underwent 3-D conformal treatment. Clinical characteristics of the patients are reported in Table 1.

Patient preparation and RG-PET/CT scanning protocol

The day before RG-PET/CT acquisition, patient compliance and set-up for gated scan was tested by positioning the patient into the gantry, on a flat table, in the same position and with the same immobilization devices for radiation treatment delivery. The respiratory curve was recorded for 12 min with a real-time position management (RPM) system (Varian Medical Systems, Palo Alto, CA, USA) to check the regularity of the breathing.

Table 1 Clinical characteristics of patients ($n = 13$)

Characteristic	
Male	6/13 (46.1 %)
Mean age, years (range)	70±12 (45–88)
Clinical disease stage (TNM)	
I	2 (15.4 %)
II	0 (0.0 %)
III	10 (76.9 %)
IV	1 (7.7 %)
Histology	
SCLC	1 (7.7 %)
NSCLC	12 (92.3 %)
Previous treatments	9/13 (69.2 %)
Radiation therapy intent	
Radical	12/13 (92.3 %)
Neoadjuvant	1/13 (7.7 %)
Type of radiation therapy	
VMAT	7/13 (53.8 %)
3-D conformal	6/13 (46.2 %)

VMAT volumetric modulated arc therapy

For PET/CT examination, patients were prepared according to common guidelines [30]. In particular, patients fasted at least 6 h before tracer administration and blood glucose was assessed immediately before tracer injection (cut-off level 170 mg/dl). Patients were intravenously injected with 4.0 MBq/kg of ^{18}F-FDG and orally hydrated in the waiting time before scanning. Approximately 60 min after injection, RG-PET/CT studies were performed with a Discovery PET/CT 600 scanner (GE Healthcare, Milwaukee, WI, USA), integrated with an RPM system. For positioning, an internal laser on the scanner and skin markers were used for geometrical alignment of the patient during RG-PET/CT acquisition. One field of view (FOV) entirely encompassing the lesions was acquired in RG mode for both PET and CT. A free-breathing, ungated helical CT scan (16 slices, 40 mA, 120 kV, slice thickness 3.72 mm, rotation 0.8 s, pitch 1.375) was extended to the entire chest and upper abdomen for the contouring of the organs at risk in PTV. RG-CT was acquired in step-and-shoot mode, 40 mA, 120 kV, rotation time 0.5 s, revolution duration equal to patient's breathing period +0.5 s, slice thickness 2.5 mm; RG-CT images were then retrospectively sorted into six phases of the respiratory cycle recorded during acquisition. RG-PET was acquired in 3-D list mode with 12 min duration; images were then retrospectively reconstructed into six breathing phases, 2 min/phase, with iterative reconstruction (ordered subset expectation maximization, OSEM), 256 matrix size, attenuation, random and scatter correction. Attenuation correction of RG-PET images was obtained from the corresponding breathing phases of RG-CT data (phase-matched attenuation correction).

PTV definition

Standard PTV definition

Free-breathing helical CT images, obtained during the PET/CT study, were transferred to the treatment planning system (TPS), an Oncentra MasterPlan 4.1 SP2 workstation (Nucletron BV, Veenendaal, The Netherlands), and standard clinical target volumes (CTV1) were manually contoured by the radiation oncologist. Standard PTV (PTV1) resulted from CTV1 with the addition of 1 cm of expansion in all directions in order to compensate for internal organ motion and set-up errors [12].

RG-PTV definition

RG-PET and RG-CT images were displayed on AW 4.6 workstation (GE Healthcare, Milwaukee, WI, USA), with preset window levels and colour scale according to a standardized institutional protocol for metabolic lesion contouring. The RG-MTV was initially obtained by an automatic segmentation algorithm commercially implemented on the workstation, with a fixed threshold of 42 % of the maximal activity of the target lesion [31]. Segmentation was performed on all images of each single phase of the patient's respiratory cycle. The nuclear medicine physician (LG) visually evaluated the automatically generated volume and, if considered inappropriate, manually corrected. In particular, physiological uptake areas (cardiac wall, chest wall, vessel activity) were carefully excluded from contouring; in cases where portions of the pathological metabolic lesion were excluded by the automatic segmentation method, they were manually included. The RG-MTV was obtained by the union of the metabolic volumes contoured on each respiratory phase of gated PET data and represents the volume in which the metabolic lesion is moving during the whole breathing cycle (i.e. the metabolic internal target volume). Then, the RG-MTV was transferred to the TPS workstation in the Radiotherapy Department.

RG-CT-based CTV (CTV2) was defined by the radiation oncologist (SM, RN) by manually contouring each CT image in all six respiratory gates. The CTV2 resulted from the union of the volumes derived from each gate. RG-CT-based PTV (PTV2) was obtained from CTV2 by adding a margin expansion of 7–8 mm in head to feet direction and 5 mm in anterior to posterior and left to right direction to compensate for set-up errors [14, 21, 32–34]. RG-PET/CT-based CTV (CTV3) was calculated by the radiation oncologist (SM, RN) by the union of CTV2 and RG-MTV. The RG-PET/CT-

based PTV (PTV3) was then obtained with the addition of the same margin expansion previously mentioned for PTV2.

The lesion displacement was also assessed on the TPS workstation by calculating the movement of the geometric centre of the lesion in all phases of RG-CT. The displacement along the x, y, z axis and total displacement vector were assessed.

Critical organs (lung, heart, spinal cord) were contoured on ungated free-breathing helical CT images. The irradiation dose was delivered to each patient on the basis of PTV3 data.

Data analysis

The paired Student's *t* test was used to assess statistical difference between CTV and PTV values. For each target lesion, the absolute and percentage differences between standard PTV1, PTV2 and PTV3 were calculated. The geometrical portion of PTV2 and PTV3 encompassed by PTV1 (intersection PTV1-PTV2 and intersection PTV1-PTV3, respectively) and the geometrical portion of PTV2 encompassed by PTV3 (intersection PTV2-PTV3) were automatically calculated on the TPS workstation as absolute and percentage values; similarly, the geometrical portion the PTV2 and PTV3 outside PTV1 (PTV2 out PTV1 and PTV3 out PTV1, respectively) and the geometrical portion of PTV2 outside PTV3 (PTV2 out PTV3) were assessed for each target lesion.

Results

Overall, 13 target lesions in 13 patients could be evaluated. Of 13 patients, 8 had nodal disease at PET/CT. In 3/13 patients (23 %) (patients 1, 6 and 13 in Table 2) nodal lesions were encompassed in target lesions as they were very close to them. In 5/13 patients (38.5 %) (patients 2, 3, 9, 11 and 12 in Table 2) nodal lesions were contoured apart and not included in CTV and PTV calculations. In Table 2 CTV and PTV values are reported for each lesion. In Table 3 the absolute and percentage differences of PTV, PTV intersection and the portion of PTVs out are reported for each lesion. The percentages of PTV2 out PTV1 and PTV3 out PTV1 were not lower than 10 % in 6/13 cases (46.2 %) and than 20 % in 3/13 cases (23.1 %). The percentage of PTV3 out PTV2 was not lower than 10 % in 3/13 lesions (23.1 %) and not lower than 20 % in only 1/13 lesions (7.7 %). In Table 4 the mean ± SD values of CTV, PTV, PTV intersection and PTVs out are reported. The CTV1 value was significantly smaller than CTV2 and CTV3, whereas no statistically significant difference was found between CTV2 and CTV3. Conversely, the PTV1 value was significantly larger than both PTV2 and PTV3, whereas PTV2 and PTV3 values did not

Table 2 CTV and PTV values for each lesion

Patient	RG-MTV (ml)	CTV (ml)			PTV (ml)		
		CTV1	CTV2	CTV3	PTV1	PTV2	PTV3
1	17.8	6.9	15.2	21.7	82.7	62.2	75.2
2	2.3	1.7	5.5	5.3	22.9	22.2	21.5
3	14.9	23.0	22.3	18.4	106.3	57.6	49.4
4	17.3	13.0	30.9	31.4	71.7	73.1	74.2
5	26.9	39.1	51.4	49.9	151.4	110.6	105.2
6	51.7	63.3	131.2	132.0	185.9	258.3	260.3
7	3.6	2.5	3.5	3.8	32.2	17.3	17.1
8	108.2	85.1	85.0	105.8	274.1	161.6	198.1
9	32.8	7.8	31.7	31.0	70.4	65.0	64.1
10	26.6	71.8	74.7	75.1	250.4	155.2	159.7
11	2.2	1.0	2.0	2.1	33.2	16.6	16.8
12	0.9	0.1	1.0	1.0	10.3	8.9	8.7
13	111.3	81.1	105.5	105.5	251.2	210.9	210.8

RG-MTV respiratory-gated metabolic tumour volume, *CTV* clinical target volume, *PTV* planning target volume, *CTV1* free-breathing helical CT-based CTV, *CTV2* RG-CT-based CTV, *CTV3* RG-PET/CT-based CTV, *PTV1* free-breathing helical CT-based PTV, *PTV2* RG-CT-based PTV, *PTV3* RG-PET/CT-based PTV

show significant differences. No statistically significant difference was found among PTV intersections and PTVs out.

In Table 5, the lung lesion dimension on CT, lesion location, lesion displacement along orthogonal directions and vector displacement are reported for each lesion. The mean (median) ± SD lesion dimension was 39.4 (38.5)± 16.5 mm. Six lesions were located in the inferior/medial lobe and seven in the superior lobe.

Discussion

Respiratory motion can affect the quality of diagnostic PET/CT imaging. The effect of motion on volume definition is particularly relevant in radiation treatment planning, as the target lesion, although detectable, can be substantially altered in shape, borders and dimension. Information on the amount and nature of the organ motion is thus essential for the determination of internal margin size and technical solution for handling respiratory motion in PET/CT, which can be essential to personalizing target volume and optimizing radiation treatment strategy [23]. The aim of this paper was to compare PTV obtained from free-breathing helical CT, commonly used for radiation therapy planning, with PTV defined by using RG-PET/CT.

Our data showed that PTV1 (free-breathing helical CT-based) was significantly larger than both PTV2 (gated CT-based) and PTV3 (gated PET/CT-based) (*p*= 0.038 and *p*=

Table 3 Absolute and percentage differences of PTV, PTV intersection and the portion of PTVs out for each lesion

Patient	PTV1–PTV2 $\left(\frac{V1-V2\%}{V1}\right)$ ml(%)	PTV1–PTV3 $\left(\frac{V1-V3\%}{V1}\right)$ ml(%)	PTV2–PTV3 $\left(\frac{V2-V3\%}{V2}\right)$ ml(%)	Intersection PTV1–PTV2 $\left(\frac{V1\cap V2\%}{V2}\right)$ ml(%)	Intersection PTV1–PTV3 $\left(\frac{V1\cap V3\%}{V3}\right)$ ml(%)	Intersection PTV2–PTV3 $\left(\frac{V2\cap V3\%}{V2}\right)$ ml(%)	PTV2 out PTV1 $\left(\frac{V2outV1\%}{V2}\right)$ ml(%)	PTV3 out PTV1 $\left(\frac{V3outV1\%}{V3}\right)$ ml(%)	PTV3 out PTV2 $\left(\frac{V3outV2\%}{V3}\right)$ ml(%)
1	20.5 (24.8)	7.5 (9.1)	−13.0 (−20.9)	52.6 (84.6)	59.0 (78.4)	58.6 (77.9)	9.6 (15.4)	16.2 (21.6)	16.6 (22.1)
2	0.7 (3.0)	1.4 (6.1)	0.7 (3.3)	16.6 (74.8)	16.3 (75.9)	21.2 (98.8)	5.6 (25.2)	5.2 (24.1)	0.3 (1.2)
3	48.7 (45.8)	56.9 (53.5)	8.2 (14.3)	56.7 (98.5)	49.3 (99.8)	48.8 (98.8)	0.9 (1.5)	0.1 (0.2)	0.6 (1.2)
4	−1.4 (−2.0)	−2.5 (−3.5)	−1.1 (−1.5)	58.9 (80.6)	59.8 (80.6)	71.6 (96.5)	14.2 (19.4)	14.4 (19.4)	2.6 (3.5)
5	40.8 (26.9)	46.2 (30.5)	5.4 (4.9)	108.9 (98.4)	104.2 (99.1)	104.7 (99.5)	1.7 (1.6)	1.0 (0.9)	0.5 (0.5)
6	−72.4 (−38.9)	−74.4 (−40.0)	−2.0 (−0.8)	163.1 (63.1)	162.6 (62.5)	247.9 (95.2)	95.2 (36.9)	97.7 (37.5)	12.4 (4.8)
7	14.9 (46.3)	15.1 (46.9)	0.2 (1.0)	17.1 (98.8)	15.9 (92.7)	14.9 (87.3)	0.2 (1.2)	1.3 (7.3)	2.2 (12.7)
8	112.5 (41.1)	76.0 (27.7)	−36.5 (−22.6)	160.0 (99.1)	184.8 (93.3)	160.6 (81.1)	1.5 (0.9)	13.3 (6.7)	37.5 (18.9)
9	5.4 (7.7)	6.3 (8.9)	0.9 (1.4)	51.6 (79.4)	51.3 (80.0)	63.3 (98.7)	13.4 (20.6)	12.8 (20.0)	0.8 (1.3)
10	95.2 (38.0)	90.7 (36.2)	−4.5 (−2.9)	139.6 (90.0)	143.2 (89.6)	153.6 (96.1)	15.6 (10.0)	16.5 (10.4)	6.2 (3.9)
11	16.6 (49.9)	16.4 (49.3)	−0.2 (−1.2)	16.3 (98.0)	16.8 (99.6)	15.3 (90.7)	0.3 (2.0)	0.1 (0.4)	1.6 (9.3)
12	1.4 (13.6)	1.6 (15.1)	0.2 (1.8)	8.3 (93.1)	8.5 (96.7)	8.6 (98.6)	0.6 (6.9)	0.3 (3.3)	0.1 (1.4)
13	40.3 (16.0)	40.4 (16.1)	0.1 (0.1)	203.4 (96.4)	203.9 (96.7)	208.2 (98.8)	7.5 (3.6)	6.9 (3.3)	2.6 (1.2)

PTV planning target volume, *RG* respiratory-gated, *PTV1* free-breathing helical CT-based PTV, *PTV2* RG-CT-based PTV, *PTV3* RG-PET/CT-based PTV, *Intersection PTV1–PTV2* PTV geometrically encompassed by both PTV1 and PTV2, *Intersection PTV1–PTV3* PTV geometrically encompassed by both PTV1 and PTV3, *Intersection PTV2–PTV3* PTV geometrically encompassed by both PTV2 and PTV3, *PTV2 out PTV1* portion of PTV2 not encompassed by PTV1, *PTV3 out PTV1* portion of PTV3 not encompassed by PTV1, *PTV3 out PTV2* portion of PTV3 not encompassed by PTV2

Table 4 Mean ± SD values of CTV, PTV, PTV intersection and PTVs out

Parameter (ml)		Mean ± SD	Range	Paired Student's *t* test *p* value
CTV	CTV1	30.5±33.2	0.1–85.1	CTV1 vs CTV2: 0.017
	CTV2	43.1±43.2	1.0–131.2	CTV1 vs CTV3: 0.009
	CTV3	44.8±45.2	1.0–132.0	CTV2 vs CTV3: 0.159
PTV	PTV1	118.7±94.1	10.3–274.1	PTV1 vs PTV2: 0.038
	PTV2	93.8±80.2	8.9–258.3	PTV1 vs PTV3: 0.043
	PTV3	97.0±83.9	8.7–260.3	PTV2 vs PTV3: 0.161
PTV intersection	PTV1-PTV2	81.0±66.2	8.3–203.4	PTV1-PTV2 vs PTV1-PTV3: 0.218
	PTV1-PTV3	82.7±69.3	8.5–203.9	PTV1-PTV2 vs PTV2-PTV3: 0.085
	PTV2-PTV3	90.6±78.8	8.6–247.9	PTV1-PTV3 vs PTV2-PTV3: 0.141
PTV out	PTV2 out PTV1	12.8±25.4	0.2–95.2	PTV1 out PTV2 vs PTV1 out PTV3: 0.085
	PTV3 out PTV1	14.3±25.9	0.1–97.7	PTV1 out PTV2 vs PTV2 out PTV3: 0.199
	PTV3 out PTV2	6.4±10.6	0.1–37.5	PTV1 out PTV3 vs PTV2 out PTV3: 0.140

RG respiratory-gated, *CTV* clinical target volume, *PTV* planning target volume, *CTV1* free-breathing helical CT-based CTV, *CTV2* RG-CT-based clinical target volume, *CTV3* RG-PET/CT-based clinical target volume, *PTV1* free-breathing helical CT-based PTV, *PTV2* RG-CT-based PTV, *PTV3* RG-PET/CT-based PTV, Intersection *PTV1-PTV2* PTV geometrically encompassed by both PTV1 and PTV2, intersection *PTV1-PTV3* PTV geometrically encompassed by both PTV1 and PTV3, intersection *PTV2-PTV3* PTV geometrically encompassed by both PTV2 and PTV3, *PTV2 out PTV1* portion of PTV2 not encompassed by PTV1, *PTV3 out PTV1* portion of PTV3 not encompassed by PTV1, *PTV3 out PTV2* portion of PTV3 not encompassed by PTV2

0.043, respectively). In a lesion by lesion analysis, PTV1 was larger than PTV2 and PTV3 in the same 11/13 (84.6 %) cases (Table 2). Compared to PTV2 and PTV3, PTV1 increase ranged from 3.0 % (Table 3, lesion 2) to 49.9 % (Table 3, lesion 11) and from 6.1 % (Table 3, lesion 2) to 53.5 %

Table 5 Lung lesion dimension on CT, lesion location, lesion displacement along orthogonal directions and vector displacement for each lesion

Patient	CT lesion dimension (mm)	Lesion location	Lesion displacement			
			Δx (mm)	Δy (mm)	Δz (mm)	ΔS (mm)
1	35	SL	0.5	1.5	3.4	3.7
2	21	ML	1.4	6.5	2.3	7.0
3	46	SL	1.4	3.2	1.7	3.9
4	39	IL	3.3	9.8	4.4	11.2
5	54	SL	2.8	3.2	5.9	7.3
6	66	IL	1.8	3.3	2.3	4.4
7	21	SL	2.8	0	2.3	3.6
8	63	IL	1.9	3.2	1.3	3.9
9	43	IL	1.5	3	3.7	5.0
10	35	SL	2.9	5.3	4.7	7.6
11	36	ML	2.2	1.4	1.1	2.8
12	12	SL	0.5	0.5	2.3	2.4
13	38	SL	1.5	0.6	6.2	6.4

SL superior lobe, *IL* inferior lobe, *ML* medial lobe, Δx, Δy, Δz and ΔS represent the lesion displacement along left to right, head to feet, anterior to posterior directions and vector displacement, respectively

(Table 3, lesion 3), respectively. These results, in particular those regarding PTV2, are comparable to those previously published by other authors [15, 25] who demonstrated a significant reduction of PTV by using RG-CT for radiation therapy planning.

Data from this study indicate that an ungated PTV larger than RG-PTV does not imply that the former geometrically envelops the latter. In the present study, in patient 2 (Table 2) PTV1, PTV2 and PTV3 were very similar (22.9, 22.2 and 21.5 ml, respectively). The differences between PTV1/PTV2 and between PTV1/PTV3 were minimal with only 0.7 (3.0 %) and 1.4 ml (6.1 %), respectively (Table 3). Conversely, the PTV2 out and PTV3 out (volumes not encompassed in PTV1) were 5.6 (25.2 %) and 5.2 ml (24.1 %), respectively (Fig. 1). A similar condition could also be found in patient 4 (Tables 2 and 3). In these two cases, although similar PTVs values were found, a portion of the RG-PTV was outside the standard PTV due to unmatched geometrical position of the volumes. As a consequence, in these two cases the possibility of missing the lesion during treatment is high if an ungated imaging technique is used, leading to a greater probability of local relapse.

In patient 3 (Table 2) PTV1 (106.3 ml) was consistently larger than both PTV2 and PTV3 (57.6 and 49.4 ml, respectively). PTV2 out and PTV3 out were only 1.5 and 0.2 %, respectively (Table 3). In this case ungated PTV is likely to envelop not only the lesion and its motion but also healthy tissue, with an increased probability of toxicity (Fig. 2). Finally, in patient 6, PTV1 (185.9 ml) was smaller than PTV2 (258.3 ml), and PTV3 (260.3 ml) with about 37 % of gated PTV outside PTV1. Again, the probability of missing
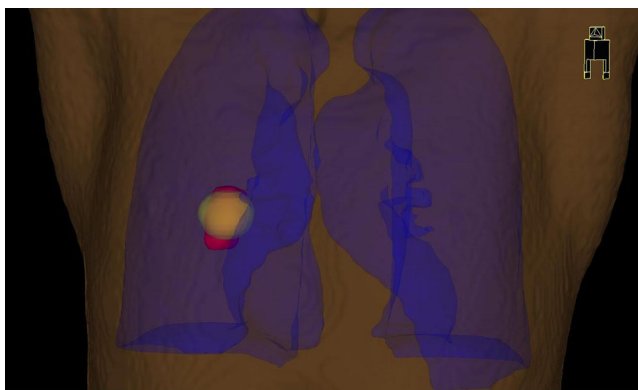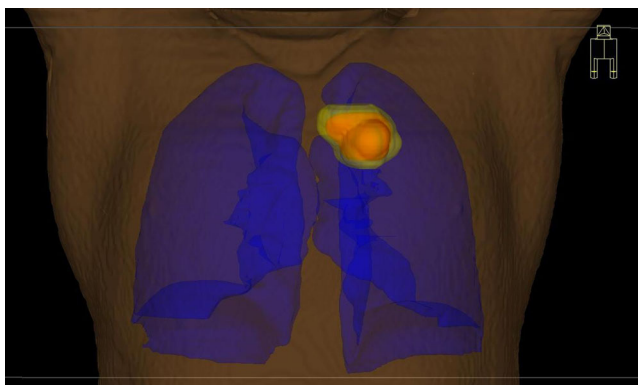
Fig. 1 Patient 2. The *yellow* and *red* volumes represent PTV1 (helical CT-based, 22.9 ml) and PTV3 (RG-PET/CT-based, 21.5 ml), respectively. There is a portion of PTV3 (5.2 ml, 24.1 %) clearly outside of PTV1

the target lesion during standard PTV-based radiation treatment could increase.

As expected, our preliminary data showed that gated CTVs were significantly larger than standard CTV (Table 4). In fact, gated CTVs were derived from gated images and included motion of the lesion during breathing. Similar results were obtained by Aristophanous et al. [29] who evaluated the clinical utility of gated metabolic imaging in radiation treatment planning and demonstrated that RG-PET-based GTV in lung lesions was significantly larger than standard PET-based GTV.

Conversely, no significant differences were found between CTV2 and CTV3 (43.1 vs 44.8 ml, $p= 0.161$), between PTV2 and PTV3 (93.8 vs 97.0 ml, $p= 0.161$) and PTV out values. Similarly, no statistically significant difference was found among PTV intersections and PTV outside regions (Table 3). Although PTV2 out PTV1 and PTV3 out PTV1 values were very similar in most of cases, in 3/13 (23.1 %) lesions (Table 3, patients 1, 7 and 8), the percentage of PTV3 out was at least 5 % higher than that of PTV2 out. Furthermore, the portion of PTV3 out PTV2 was at least higher than 10 % in

Fig. 2 Patient 3. The *yellow* and *orange* volumes represent PTV1 (helical CT-based, 106.3 ml) and PTV3 (RG-PET/CT-based, 49.4 ml), respectively. PTV1 is larger than RG-PTV and includes a portion of healthy tissues

3/13 (23.1 %) cases (Table 3, patients 1, 7 and 8). Currently these data cannot be used to draw conclusions and need to be confirmed in a larger population, but they could indicate that RG-PET/CT can add useful information to RG-CT for a better definition of the target volume in some cases.

In our study, lesion displacement did not correlate with PTV values. In particular, the lesions with the highest values of motion vector ΔS (patients 4, 5 and 10 in Table 5) showed different values of PTV2 out and PTV3 out, ranging from 19.4 % for lesion 4 to only 0.9 % (PTV3 out) for lesion 5. Furthermore, the lesion (patient 6) with the highest percentage of PTV3 out (37.5 %) showed a ΔS value of only 4.4 mm. This variability could be related to the lack of predictability of motion based on lesion location in our patients. The standard CTV expansion could thus be inappropriate to correctly define the internal target volume of the lesion.

In the present work, different margins of expansion have been applied to obtain standard and gated PTV. Consequently, it can be argued that the differences found in PTV values could be related to the different methodology rather than to the imaging techniques. However, when CTV is obtained from free-breathing CT, the lack of information on lesion motion forces the use of internal margins, in addition to set-up margins, to compensate for an uncertain and estimated motion and to reduce the risk of missing the lesion during treatment delivery. Conversely, when lesion motion is managed with a gated imaging technique, CTV can encompass the volume in which the lesion is moving during breathing (i.e. internal volume) and it is usually larger than standard CTV as found in our work; nevertheless, only set-up margins have to be added to CTV because internal margins have been already included [35]. Accordingly, the different margins of expansion used in the present work for PTV assessment can be considered strictly related to the imaging technique used for radiation treatment planning and reflects what is commonly performed in clinical practice. Although probably of interest from a merely investigational point of view, the use of the same margin expansion independently from the imaging technique cannot be considered a valid approach when translated into the clinical routine of radiation treatment planning [12].

Another issue in the present work is the use of anisotropic expansion in gated PTVs, with 5 mm in left to right and anterior to posterior directions and 7–8 mm in head to feet direction. The larger expansion in head to feet direction was not arbitrary and it was used because usually head to feet is the direction with both the larger motion [14, 21, 32, 33] and more consistent interfractional motion variability during radiotherapy courses [34]. Although a gating imaging technique is used, both factors can generate uncertainty in volume definition that can be compensated for by larger margin expansion in head to feet direction. In addition, a margin expansion of 7 and 8 mm was used for lesions located

in the superior and medial-inferior lobe, respectively, as the lesion location can be correlated to different motion amplitude in head to feet direction [12, 14, 21, 34].

In the present work, the contouring of gated PET images was performed by the same nuclear medicine physician (LG) with an automated commercial software implemented on the workstation. PTVs were always manually defined by the same two radiation oncologists (SM, RN). Although the inter-observer variability in volume definition was not evaluated as it was not the aim of the present study, it is recognized that inter-physician GTV variation can have important dosimetric consequences, often more important than those of respiratory motion [12]. Notwithstanding, it has to be considered that all physicians involved in the processing of the data of this paper are well experienced in image contouring (more than 7 years) for radiation treatment planning and followed institutional standardized protocols.

In the present study, only one method was applied for contouring of PET images [31], as it has been the method commonly used in routine clinical practice for many years in our institution and commercially implemented in the workstation used for contouring. A comparison of different segmentation algorithms, although of interest, was not performed as it was not a matter of the investigation. Moreover, it has to be considered that to date there is no standard reference for metabolic target lesion contouring [36] and the manual procedure can also be considered a valid approach when methodology is standardized [37].

Compared to a standard scan, RG techniques are time consuming and require more time for scanner and patient set-up, acquisition and processing of data. Nevertheless, modern PET/CT scanners are commercially implemented with gating tools and powerful hardware and software capabilities that enable RG studies yet reduce the time for acquisition and processing data. This can be a positive impacting factor to further encourage the use of gating techniques in routine clinical practice. Furthermore, a single axial or helical planning CT scan acquired during free breathing is not an optimal study, because it may capture the random position of a tumour and/or generate artefacts of the patient's anatomy. Planning on scans that are not representative of the tumour position during the time of the delivery of radiotherapy may result in systematic errors. Consequently, the use of a gating technique is strongly recommended for treatment planning in thoracic oncology, in spite of the need to deal with methodological issues [20].

A limitation of this study is the small sample size. However, while these are only preliminary data, they indicate the strength of a gating technique to optimize the radiation treatment planning in lung cancer patients. Secondly, another limitation of the study is the lack of comparison between PTV based on standard PET/CT and RG-PET/CT. However, the aim of our work was to compare a motion handling technique to the commonly used standard CT-based procedure for PTV definition. Finally, we cannot provide patient outcomes derived from the use of RG-PET/CT in radiation treatment planning as this was not a specific matter of investigation and also due to the limited number of patients analysed.

In conclusion, our preliminary data indicate that the use of RG-PET/CT in lung cancer can affect not only the volume of PTV but also its shape. When gated PET/CT information was added to gated CT, PTV changed in about 23 % of cases. The use of a gating technique is thus crucial for better delineating PTV by tailoring the target volume to the lesion motion.

References

1. Nestle U, Walter K, Schmidt S, Licht N, Nieder C, Motaref B, et al. 18F-deoxyglucose positron emission tomography (FDG-PET) for the planning of radiotherapy in lung cancer: high impact in patients with atelectasis. Int J Radiat Oncol Biol Phys 1999;44(3):593–7.
2. Mah K, Caldwell CB, Ung YC, Danjoux CE, Balogh JM, Ganguli SN, et al. The impact of (18)FDG-PET on target and critical organs in CT-based treatment planning of patients with poorly defined non-small-cell lung carcinoma: a prospective study. Int J Radiat Oncol Biol Phys 2002;52(2):339–50.
3. Bradley J, Thorstad WL, Mutic S, Miller TR, Dehdashti F, Siegel BA, et al. Impact of FDG-PET on radiation therapy volume delineation in non-small-cell lung cancer. Int J Radiat Oncol Biol Phys 2004;59(1):78–86. doi:10.1016/j.ijrobp.2003.10.044.
4. MacManus M, Nestle U, Rosenzweig KE, Carrio I, Messa C, Belohlavek O, et al. Use of PET and PET/CT for radiation therapy planning: IAEA expert report 2006–2007. Radiother Oncol 2009;91(1):85–94. doi:10.1016/j.radonc.2008.11.008.
5. Nehmeh SA, Erdi YE, Ling CC, Rosenzweig KE, Schoder H, Larson SM, et al. Effect of respiratory gating on quantifying PET images of lung cancer. J Nucl Med 2002;43(7):876–81.
6. Nehmeh SA, Erdi YE, Ling CC, Rosenzweig KE, Squire OD, Braban LE, et al. Effect of respiratory gating on reducing lung motion artifacts in PET imaging of lung cancer. Med Phys 2002;29(3):366–71.
7. Erdi YE, Nehmeh SA, Pan T, Pevsner A, Rosenzweig KE, Mageras G, et al. The CT motion quantitation of lung lesions and its impact on PET-measured SUVs. J Nucl Med 2004;45(8):1287–92.
8. Osman MM, Cohade C, Nakamoto Y, Wahl RL. Respiratory motion artifacts on PET emission images obtained using CT attenuation correction on PET-CT. Eur J Nucl Med Mol Imaging 2003;30(4):603–6. doi:10.1007/s00259-002-1024-x.
9. Pan T, Mawlawi O, Nehmeh SA, Erdi YE, Luo D, Liu HH, et al. Attenuation correction of PET images with respiration-averaged CT images in PET/CT. J Nucl Med 2005;46(9):1481–7.
10. Mawlawi O, Pan T, Macapinlac HA. PET/CT imaging techniques, considerations, and artifacts. J Thorac Imaging 2006;21(2):99–110.
11. Bowen SR, Nyflot MJ, Gensheimer M, Hendrickson KR, Kinahan PE, Sandison GA, et al. Challenges and opportunities in patient-specific, motion-managed and PET/CT-guided radiation therapy of lung cancer: review and perspective. Clin Transl Med 2012;1(1):18. doi:10.1186/2001-1326-1-18.

12. Keall PJ, Mageras GS, Balter JM, Emery RS, Forster KM, Jiang SB, et al. The management of respiratory motion in radiation oncology report of AAPM Task Group 76. Med Phys 2006;33(10):3874–900.

13. Colgan R, McClelland J, McQuaid D, Evans PM, Hawkes D, Brock J, et al. Planning lung radiotherapy using 4D CT data and a motion model. Phys Med Biol 2008;53(20):5815–30. doi:10.1088/0031-9155/53/20/017.

14. Guckenberger M, Wilbert J, Krieger T, Richter A, Baier K, Flentje M. Mid-ventilation concept for mobile pulmonary tumors: internal tumor trajectory versus selective reconstruction of four-dimensional computed tomography frames based on external breathing motion. Int J Radiat Oncol Biol Phys 2009;74(2):602–9. doi:10.1016/j.ijrobp.2008.12.062.

15. Hof H, Rhein B, Haering P, Kopp-Schneider A, Debus J, Herfarth K. 4D-CT-based target volume definition in stereotactic radiotherapy of lung tumours: comparison with a conventional technique using individual margins. Radiother Oncol 2009;93(3):419–23. doi:10.1016/j.radonc.2009.08.040.

16. Underberg RW, Lagerwaard FJ, Slotman BJ, Cuijpers JP, Senan S. Benefit of respiration-gated stereotactic radiotherapy for stage I lung cancer: an analysis of 4DCT datasets. Int J Radiat Oncol Biol Phys 2005;62(2):554–60. doi:10.1016/j.ijrobp.2005.01.032.

17. Wolthaus JW, Schneider C, Sonke JJ, van Herk M, Belderbos JS, Rossi MM, et al. Mid-ventilation CT scan construction from four-dimensional respiration-correlated CT scans for radiotherapy planning of lung cancer patients. Int J Radiat Oncol Biol Phys 2006;65(5):1560–71. doi:10.1016/j.ijrobp.2006.04.031.

18. Wolthaus JW, Sonke JJ, van Herk M, Belderbos JS, Rossi MM, Lebesque JV, et al. Comparison of different strategies to use four-dimensional computed tomography in treatment planning for lung cancer patients. Int J Radiat Oncol Biol Phys 2008;70(4):1229–38. doi:10.1016/j.ijrobp.2007.11.042.

19. Wolthaus JW, Sonke JJ, van Herk M, Damen EM. Reconstruction of a time-averaged midposition CT scan for radiotherapy planning of lung cancer patients using deformable registration. Med Phys 2008;35(9):3998–4011.

20. De Ruysscher D, Faivre-Finn C, Nestle U, Hurkmans CW, Le Péchoux C, Price A, et al. European Organisation for Research and Treatment of Cancer recommendations for planning and delivery of high-dose, high-precision radiotherapy for lung cancer. J Clin Oncol 2010;28(36):5301–10. doi:10.1200/JCO.2010.30.3271.

21. Liu HH, Balter P, Tutt T, Choi B, Zhang J, Wang C, et al. Assessing respiration-induced tumor motion and internal target volume using four-dimensional computed tomography for radiotherapy of lung cancer. Int J Radiat Oncol Biol Phys 2007;68(2):531–40. doi:10.1016/j.ijrobp.2006.12.066.

22. Underberg RW, Lagerwaard FJ, Slotman BJ, Cuijpers JP, Senan S. Use of maximum intensity projections (MIP) for target volume generation in 4DCT scans for lung cancer. Int J Radiat Oncol Biol Phys 2005;63(1):253–60. doi:10.1016/j.ijrobp.2005.05.045.

23. Korreman S, Persson G, Nygaard D, Brink C, Juhler-Nøttrup T. Respiration-correlated image guidance is the most important radiotherapy motion management strategy for most lung cancer patients. Int J Radiat Oncol Biol Phys 2012;83(4):1338–43. doi:10.1016/j.ijrobp.2011.09.010.

24. Paumier A, Crespeau A, Krhili S, Georgin-Mège M, Tuchais C, Mesgouez J, et al. Dosimetric study of the different techniques to deal with respiratory motion for lung stereotactic radiotherapy. Cancer Radiother 2012;16(4):263–71. doi:10.1016/j.canrad.2012.03.004.

25. Rietzel E, Liu AK, Doppke KP, Wolfgang JA, Chen AB, Chen GT, et al. Design of 4D treatment planning target volumes. Int J Radiat Oncol Biol Phys 2006;66(1):287–95. doi:10.1016/j.ijrobp.2006.05.024.

26. Lupi A, Zaroccolo M, Salgarello M, Malfatti V, Zanco P. The effect of 18F-FDG-PET/CT respiratory gating on detected metabolic activity in lung lesions. Ann Nucl Med 2009;23(2):191–6. doi:10.1007/s12149-008-0225-1.

27. García Vicente AM, Soriano Castrejón AM, Talavera Rubio MP, León Martín AA, Palomar Muñoz AM, Pilkington Woll JP, et al. 18F-FDG PET-CT respiratory gating in characterization of pulmonary lesions: approximation towards clinical indications. Ann Nucl Med 2010;24(3):207–14. doi:10.1007/s12149-010-0345-2.

28. Guerra L, De Ponti E, Elisei F, Bettinardi V, Landoni C, Picchio M, et al. Respiratory gated PET/CT in a European multicentre retrospective study: added diagnostic value in detection and characterization of lung lesions. Eur J Nucl Med Mol Imaging 2012;39(9):1381–90. doi:10.1007/s00259-012-2148-2.

29. Aristophanous M, Berbeco RI, Killoran JH, Yap JT, Sher DJ, Allen AM, et al. Clinical utility of 4D FDG-PET/CT scans in radiation treatment planning. Int J Radiat Oncol Biol Phys 2012;82(1):e99–e105. doi:10.1016/j.ijrobp.2010.12.060.

30. Boellaard R, O'Doherty MJ, Weber WA, Mottaghy FM, Lonsdale MN, Stroobants SG, et al. FDG PET and PET/CT: EANM procedure guidelines for tumour PET imaging: version 1.0. Eur J Nucl Med Mol Imaging 2010;37(1):181–200.

31. Erdi YE, Mawlawi O, Larson SM, Imbriaco M, Yeung H, Finn R, et al. Segmentation of lung lesion volume by adaptive positron emission tomography image thresholding. Cancer 1997;80(12 Suppl):2505–9.

32. Ekberg L, Holmberg O, Wittgren L, Bjelkengren G, Landberg T. What margins should be added to the clinical target volume in radiotherapy treatment planning for lung cancer? Radiother Oncol 1998;48(1):71–7.

33. Seppenwoolde Y, Shirato H, Kitamura K, Shimizu S, van Herk M, Lebesque JV, et al. Precise and real-time measurement of 3D tumor motion in lung due to breathing and heartbeat, measured during radiotherapy. Int J Radiat Oncol Biol Phys 2002;53(4):822–34.

34. Sonke JJ, Lebesque J, van Herk M. Variability of four-dimensional computed tomography patient models. Int J Radiat Oncol Biol Phys 2008;70(2):590–8. doi:10.1016/j.ijrobp.2007.08.067.

35. ICRU. International Commission on Radiation Units and Measurements. Prescribing, recording and reporting photon beam therapy. In: ICRU Report 62. J. ICRU. Oxford: Oxford University Press

36. Lee JA. Segmentation of positron emission tomography images: some recommendations for target delineation in radiation oncology. Radiother Oncol 2010;96(3):302–7. doi:10.1016/j.radonc.2010.07.003.

37. Bayne M, Hicks RJ, Everitt S, Fimmell N, Ball D, Reynolds J, et al. Reproducibility of "intelligent" contouring of gross tumor volume in non-small-cell lung cancer on PET/CT images using a standardized visual method. Int J Radiat Oncol Biol Phys 2010;77(4):1151–7. doi:10.1016/j.ijrobp.2009.06.032.